Original Article

OPEN ACCESS

Numerical 3D Model of Suspended Sediment Transport Downstream Al-Amarah Barrage, Iraq

Abaas J. Ismaeel [1,*], Sarmad A. Abbas [2], Wisam S. Al-Rekabi [3]

[1,2,3] *Department of Civil Engineering, College of Engineering, University of Basrah, Basrah, Iraq*
E-mail addresses: jabbaas@yahoo.com , sarmad.abbaas@uobasrah.edu.iq , wisam.neaamah@uobasrah.edu.iq

Abstract

This research is an analytical study for simulation both sediment transport and flow within the Tigris river reach located downstream of the Al-Amarah barrage within the Maysan province. This study adopted a three-dimensional program (SSIIM) which use the Navier-Stokes equations for calculating the flow, and the convection-diffusion equations for calculating the sediment transport by the finite volume method as approximated method. A structured non-orthogonal three-dimensional grid is employed to perform the simulation. The obtained results are subsequently compared to the field measurements. The determination coefficient (R^2) for this comparison is 0.96 for flow velocity distribution and 0.94 for sediment concentration distribution. The results also showed through the simulation of the water flow, the state of the secondary flow and its effect on both the main flow and the erosion of the river bed in the studied cross sections. According to the high convergence of the results of this model with the field measurements, this model is a powerful tool for simulating flow and sediment concentrations in river systems and channels.

Keywords: Numerical Model SSIIM, Al-Amarah Barrage, Secondary Flow, Navier Stokes, Suspended Sediment Transport.

1. Introduction

When water flows in natural channels and rivers, it will lead to the sedimentation processes, included morphological changes. Sediment transport and morphological aspects have a very great engineering and economic importance, and an example of this is the assessment of the impact of bank erosion risks on near bank properties in addition to the loss that occurs in important parts of the lands which are often invested in agriculture, estimating the quantities of silting due to the storage process and its effects on the morphological changes in rivers, are often have the direct impact on the hydraulic performance of the river reaches especially these located downstream of dams and barrages. These and other reasons, and the failure to properly predict the sediments transport behavior and their quantities, have led to many problems, including the collapse of bridges as a result of erosion of the pier foundations, the destruction of dams and banks and the increase in the quantities of sand dunes in the waterways and rivers that are navigable [1].

Hence, there is a crucial need to study the movement of sediments and predict their quantities. Towards that aim, the process of simulating sediment transport and estimating its annual quantities using computer programs is a good way to do. In recent years, many mathematical models have been developed to simulate the three-dimensional flow and sediment movement. Khosronejad et al. [2] conducted a laboratory simulation of sediment transport and water flow in curved open channel at 90° and 135°). The obtained experimental data was subsequently simulated using a 3D

numerical model. The obtained results, showed good agreement based on the comparison of the results of the numerical model and the measured data. Atya [3] studied the transport of sediments and their effects on the Rosaries dam by using a 3D numerical model (SSIIM). Three types of sediments were simulated depending on their diameters. The simulation results showed a concentration of suspended sediments and velocity vectors in the three directions, and demonstrated the longitudinal distributions of both the flow velocity and the concentration of suspended sediments. Ali et al. [4] used the 3-D program (SSIIM) to simulate the velocity of flow and sediment concentration of the Tigris river within Baghdad governorate, and along 18 km over 16 cross sections. The (SSIIM) model was used to predict the morphology of a river and also, through this study the annual quantities of deposition were calculated and was equal to (2.12) million tons. Mohammad et al. [5] applied a three-dimensional model (SSIIM) to study the cases of flow and sediment deposition in the Mosul Dam reservoir in Iraq, to perform the simulation the deposited load was assumed after 25 years of operation. A comparison was made between the sediment concentrations measured at several points with the simulation results as the results were logical and compatible. Therefore, the study concluded that the model performance was good in predicting the sediment load.

The reasons for choosing this study area; the lack of any data related to sediments in this study area in addition to, the lack of stations to monitor nature, quantities of sediments, and it concentrations.

In this research, a three-dimensional numerical model was developed using the (SSIIM) program to simulate the flow velocities of water and the concentration of suspended sediments for the study area located (downstream Al-Amarah barrage on the Tigris river-southern Iraq) through 20 cross sections distributed along the study area.

2. Study region

The length of the study area (at downstream Al-Amarah barrage) is about 5 km and the average width of the river is 71.9 m, and it is located between two longitudes (47.15° E and 47.145° E) and two latitudes (31.855° N and 31.805° N), as shown in the Fig. 1. Al-Amarah barrage is located on the Tigris river in the center of Maysan governorate. The purpose of constructing the barrage was to regulate the irrigation water and raise the water level at the upstream of the barrage to increase the water quantities of Al-Kahlaa, Al-Msharah and Al-Bterah rivers. This barrage consists of six radial gates of width 8 m and height 6 m. These gates are operated manually and electrically, also the downstream of this barrage consists of a navigation lock of 165 m in length and 20 m in width and contains two gates as well as a fish channel with a width of 3.5 m, as shown in Fig. 2.
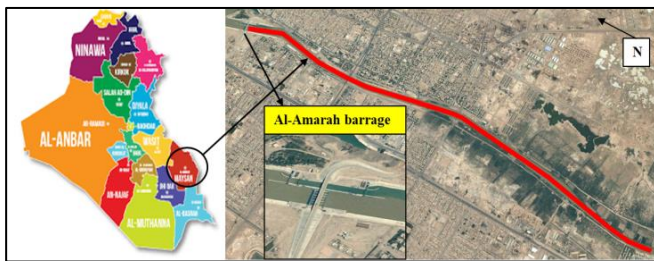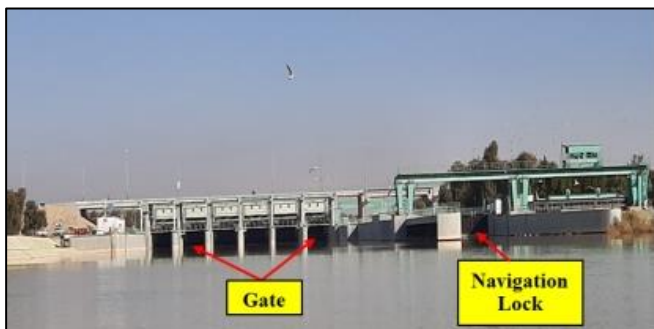

Fig. 1 Location of study region.

Fig. 2 Downstream of Al-Amarah barrage.

3. The numerical model (SSIIM)

The numerical model (SSIIM) is one of the software's of computational fluid dynamic (CFD), it is specialized in simulating sediments in a riverine environment with a complex geometry. The software contains several options, including calculating suspended sediment concentration, bed load, and velocity of flow etc. that occur in rivers and channels. The software calculates the distributions of velocity of flow by solving the Navier-Stokes equations in the (x, y, and z) directions through the turbulence model (k-e), this simulation occurs through three-dimensional grid. The calculations of sediment concentration are performed using the calculated flow velocity to solve the convection-diffusion equations [6].

3.1. Calculation of water flow

The Navier Stokes equations in the three dimensions (x, y, and z) of turbulent flow and by using the model (k-ε) have been adopted in SSIIM to calculate the turbulent shear stress, the type of turbulence model is chosen by using a data set (F 24) in the control file, (F 24) it is a code through which the software identifies the type of turbulence model used depending on the integer number that comes after it. If it is zero, this means the software will use the mentioned model. These equations are solved using the principle of control volume and as for the convective terms, second order upwind scheme or power law scheme are used to discretization them through a set of data (F 6) in the control file.

For flows with constant density and that are non-compressible, the Navier- Stokes equations can be modeled as in Eq. (1) [7]:

$$\frac{\partial U_i}{\partial t} + U_j \frac{\partial U_i}{\partial X_j} = \frac{1}{\rho} \frac{\partial}{\partial X_j}\left(-P\,\delta_{ij} - \rho\,\overline{u_i u_j}\right) \tag{1}$$

Where, U is the time-averaged velocity in three directions and (i =1, 2, and 3), u is the velocity fluctuation, P is the pressure, X_j is the Cartesian space coordinates, δ_{ij} is the Kronecker delta where (i, j) is variables number and ρ is the fluid density.

The Kronecker delta in mathematics equals:

$$\delta_{ij} = \begin{cases} 0 & \text{if } i \neq j \\ 1 & \text{if } i = j \end{cases} \tag{2}$$

From the left side of the equation, the first term is the transient term and the latter term is the convective term. From the right-hand side of the equation, the first term is the pressure and the second term is the Reynolds stress.

3.1.1. The Boussinesq approximation

The Reynolds stress term ($\overline{u_i u_j}$) can be modeled using the Boussinesq approximation, as shown in Eq. (3):

$$-\overline{u_i u_j} = \vartheta_T \left(\frac{\partial U_i}{\partial X_j} + \frac{\partial U_j}{\partial U_i}\right) \tag{3}$$

From the right side of the Eq. (3), the first term denotes the diffusive term in the Navier-Stokes equation.

3.1.2. Turbulence model (k-ε)

The k-ε model consists of two parts: k represents turbulent kinetic energy and ε represents dissipation rate which are used to calculate the eddy-viscosity [8]:

$$\vartheta_T = C_\mu\,\rho\,\frac{k^2}{\varepsilon} \tag{4}$$

$$k = \frac{1}{2}\,\overline{u_i u_j} \tag{5}$$

$$\varepsilon = \vartheta\,\frac{\overline{\frac{\partial u_i}{\partial X_j}\frac{\partial u_j}{\partial X_i}}}{} \tag{6}$$

Where, ϑ is the kinematic viscosity of the fluid.

The turbulent kinetic energy k and dissipation rate ε can be modeled as in Eq. (7) and (8):

$$\frac{Dk}{Dt} = \frac{1}{\rho} \frac{\partial}{\partial X_k} \left[\frac{\mu_T}{\sigma_k} \frac{\partial k}{\partial X_k} \right] + \frac{\mu_T}{\rho} \left(\frac{\partial U_i}{\partial X_k} + \frac{\partial U_k}{\partial X_i} \right) \frac{\partial U_i}{\partial X_k} - \varepsilon \qquad (7)$$

$$\frac{D\varepsilon}{Dt} = \frac{1}{\rho} \frac{\partial}{\partial X_k} \left[\frac{\mu_T}{\sigma_\varepsilon} \frac{\partial \varepsilon}{\partial X_k} \right] + \frac{C_1 \mu_T}{\rho} \frac{\varepsilon}{k} \left(\frac{\partial U_i}{\partial X_k} + \frac{\partial U_k}{\partial X_i} \right) \frac{\partial U_i}{\partial X_k} - C_2 \frac{\varepsilon^2}{k} \qquad (8)$$

The values of the constants shown in Eq. (4), Eq. (7) and Eq. (8) for model k-ε are [9]:

$C_\mu = 0.09$, $C_1 = 1.44$, $C_2 = 1.92$, $\sigma_k = 1$ and $\sigma_\varepsilon = 1.3$.

3.1.3. Wall laws

Wall law is employed when the velocity's gradient towards a wall is steep; it entails the turbulence equation and the Navier-Stokes equation, both of which have source terms. The wall law is used on cells near the wall in order to extract the source terms analytical expressions. In terms of flow velocity, the wall law is used to calculate the walls shear stresses. The shear stresses are then multiplied to the side area of the cell near the wall, thus representing the sink term in the velocity equation. In the SSIIM model, the wall law for rough walls is given by the empirical formula as shown in Eq. (9) [10]:

$$\frac{U(z)}{U_*} = \frac{1}{k} ln \left(\frac{30\,y}{k_s} \right) \qquad (9)$$

Where, U_* is the shear velocity (m/s), k is the constant equal to 0.4, y is the distance to the wall (m), k_s is the roughness (m) which can be determined in the (F 16) dataset in the control file. In the SSIIM model, for smooth boundaries the wall laws can be applied using the (F 15 5) dataset in the control file.

3.2. Calculation of sediment flow

Sediment transport calculation in the SSIIM program entails all the size fractions using a dataset (S) in the control file, with specifications of the fall velocity and diameter of each size fraction. The number of size fractions for sediment is determined through a data set ($G1$).

The data set ($G1$) is defined by four integers, through it, the total number of cross-sections, as well as the number of grid lines in directions (y and z), in addition to the number of sediment sizes used are known, in this study the data set ($G1$) used ($G1$ 1001 21 11 4). While the data set (S) used in this study is made up of four groups, where it was (S 1, S 2, S 3 and S 4), depending on the number of sediment sizes used.

There are two methods for entering the sediment flow into the control file. The first method entails the use of dataset (I); the Hunter-Rouse equation is used for each size fraction to attain the vertical sediment distribution via sediment concentration for the entire cross-section at the upstream of the grid i.e., ($i = 1$). The second method entails the usage of dataset (G 5) which also involves the sediment concentration for each size fraction at a specific surface of the grid's boundary [6].

3.2.1. The theory used for calculating sediment flow

The SSIIM model solves the convection-diffusion equation to calculate the suspended sediment load for sediment concentration as shown in Eq. (10):

$$\frac{\partial c}{\partial t} + U_j \frac{\partial c}{\partial X_j} + w \frac{\partial c}{\partial X_j} = \frac{\partial}{\partial X_j} \left(\Gamma \frac{\partial c}{\partial X_j} \right) + S \qquad (10)$$

Where, w is the fall velocity for particles (m/s), c is the sediment concentration, S is the source term and Γ is the diffusion coefficient that can be determined from the (k-ε) model through eddy viscosity:

$$\Gamma = \frac{\vartheta_T}{S_c} \qquad (11)$$

Where, S_c is the number of Schmidt, equaling to 1 as default, and of which can be given a different value in the (F 12) dataset in the control file.

In the SSIIM program, the equation introduced by Van Rijns (1987) is employed to calculate the equilibrium of bed concentration. This equation has several empirical parameters (i.e. 0.015, 1.5 and 0.3) which are changeable using dataset (F 6) in the control file. The Van Rijns equation is shown in Eq. (12) [11]:

$$c = 0.015 \frac{d_{50}}{a} \frac{T^{1.5}}{D_*^{0.3}} \qquad (12)$$

in which,

$$D_* = d_{50} \left(\frac{\Delta g}{\vartheta^2} \right)^{1/3} \qquad (13)$$

$$T = \frac{\bar{\tau}_b{}' - \bar{\tau}_{b,cr}}{\bar{\tau}_{b,cr}} \qquad (14)$$

$$\bar{\tau}_b{}' = \mu\,\bar{\tau}_b \qquad (15)$$

$$\bar{\tau}_b = \frac{1}{8} \rho\,f\,(\bar{v}_r)^2 \qquad (16)$$

$$\mu = \frac{f'}{f} \qquad (17)$$

$$f' = 0.24 \left[\log \left(\frac{12\,h}{3\,d_{90}} \right) \right]^{-2} \qquad (18)$$

$$f = 0.24 \left[\log \left(\frac{12\,h}{k_s} \right) \right]^{-2} \qquad (19)$$

$$\bar{v}_r = (\bar{u}^2 + \bar{v}^2)^{0.5} \qquad (20)$$

$$\Delta = \frac{\rho_s - \rho}{\rho} \qquad (21)$$

Where D_* is the parameter of particle size, T is the parameter of transport stage, $\bar{\tau}_b{}'$ is the effective shear stress of bed in (N/m²), $\bar{\tau}_b$ is the current related shear stress of bed in (N/m²), $\bar{\tau}_{b,cr}$ is the critical shear stress of bed at inception of motion in (N/m²), a is the reference level in (m), μ is the factor for bed form, f' is the grain friction factor, f is the overall friction factor, $\bar{v}_r$ is the depth average of velocity vector in

(m/s), h is the depth of water in (m), k_s is the roughness height of bed in (m), and Δ is the relative density.

The height of the bed form is calculated using the Van Rijns equation:

$$\frac{\Delta_b}{h} = 0.11 \left(\frac{d_{50}}{h}\right)^{0.3} (1 - e^{-0.5\,T})(25 - T) \qquad (22)$$

The roughness of the height of the bed form k_s is calculated using the Eq. (23):

$$k_s = 3\,d_{90} + 1.1\,\Delta_b \left(1 - e^{\frac{-25\,\Delta_b}{\lambda_b}}\right) \qquad (23)$$

Where Δ_b is the height of the bed form, λ_b is the length of the bed form equal to $7.3\,h$.

4. Field Measurements

The field Measurements in this study included the collection of data from the cross sections, which are represented by the hydraulic properties data for the study area and the suspended sediment properties data, in addition to collecting samples from the river bed, as explained herein:

4.1. Determination of cross-sections in study reach

A total of 20 cross-sections with a 250 m distance in between have been conducted along the study area; the length of study area is about 5 km towards the downstream of the Al-Amarah barrage as illustrated in Fig. 3. The cross-sections geometric data is used to construct a mesh for the study area using the SSIIM model and as the model's input data.

Fig. 3 Cross-section locations for the study reach.

4.2. Hydraulic and geometric data measurements

The Acoustic Doppler Current Profiler (ADCP) device is used to obtain hydraulic and geometric data for the cross-sections which are denoted as water flow velocity, water discharge, water surface width and cross-sectional geometry. Figure 4 presents the geometry of cross-section No 3. All data obtained are tabulated in Table 1.
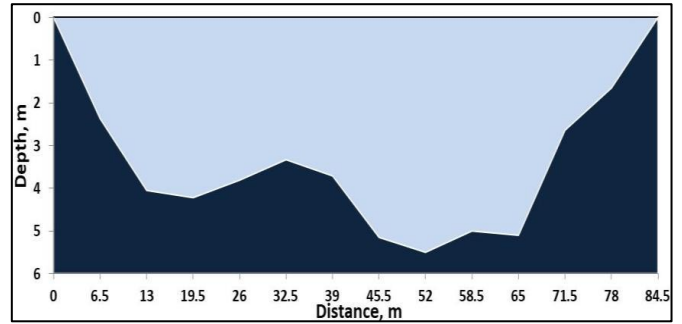

Fig. 4 Geometry of cross-section No. 3.

Table 1. Hydraulic properties for all sections.

Section No.	Max. depth (m)	Average velocity (m/s)	Total area (m²)	Discharge (m³/s)
1	5.67	0.32	392.6	123.95
2	4.81	0.32	388.9	124.87
3	5.46	0.42	306.4	127.33
4	4.94	0.42	296.9	126.02
5	5.46	0.39	317.3	123.60
6	5.77	0.49	254.2	124.72
7	6.28	0.44	279.2	124.12
8	5.24	0.48	256.4	122.65
9	4.76	0.44	274.7	120.30
10	4.29	0.42	276.0	117.10
11	4.38	0.41	287.3	117.94
12	6.32	0.46	251.5	116.23
13	5.74	0.45	261.2	116.63
14	5.36	0.47	242.1	113.63
15	4.21	0.45	248.6	112.05
16	3.82	0.44	259.4	114.77
17	4.72	0.49	229.1	111.18
18	6.01	0.49	225.1	110.89
19	6.22	0.49	218.4	108.00
20	5.15	0.49	214.8	104.92

4.3. Sampling of suspended sediment

Suspended sediments in the channels and rivers are examined by obtaining their samples via a number of methods including depth integrating sampler, point integrating sampler, and pumping samplers. The point integrating sampler is employed in this study using a homemade device.

4.4. Sampling of bed material

The river bed samples are taken using the Van Veen grab sampler. The researcher manufactured a device which has a similar shape, dimensions and weight to the common Van Veen grab sampler. It is considered as an effective riverine sampling tool [12]. Three samples are taken from the bed of each cross-section at (1/4, 1/2, and 3/4) from the top width of each cross-section. The samples are then mixed to obtain a homogeneous sample representing the bed material of each cross-section, following which a sample is extracted for laboratory analysis [13], [14].

5. Laboratory Tests

The laboratory tests include data of the concentration and discharge of suspended sediments for the study area and for each cross-section, data of the sediment distribution curves via hydrometer testing and sieve analysis of the bed materials, and values of specific gravity. These are treated as input data for running the SSIIM model, as detailed in the following sub-sections:

5.1. Concentration of suspended sediment

The suspended sediment concentrations are attained in the lab by filtering the samples using the filtration method. As for the sampling sites, the point integrating method is used which to determine the vertical distribution of the suspended sediments. This method includes dividing the surface width of the river into three columns (1/4, 1/2, and 3/4). For each cross-section, three samples are taken from each column (0.2d, 0.6d, and 0.8d) where d represents the depth of water measured from the surface; there are nine samples in each cross-section [15]. The minimum and maximum of the suspended sediment concentrations are 56 and 153.1 mg/l, respectively.

Regarding the sampling device consists of one liter plastic bottles. Two holes were drilled in the cap of each bottle and copper tubes (8 mm) were inserted into each hole about (3 cm) in the bottle (air exhaust pipe and intake tube). The area around the tube is sealed with a sealing material to ensure no water leaks into the bottle and to prevent the tubing from sliding in and out of the bottle cap. Many of these units can be installed in one station (three bottles are installed on the fencepost). Entrances to the samples were at varying depths depending on the depth of the column, so that sediment samples can be collected from different depths inside the water column. The mixture of water and sediments enters as the water level rises to the height at which the intake tube was placed. Bottles placed in positions where samples are obtained. This sampler gradually fills.

5.2. Grain sizes distribution and specific gravity of bed materials

The sediment distribution curve for each cross-section is obtained via the sieve and hydrometer analyses of the river bed samples for the study area using the ASTM D422 [16] standard as in Fig. 5. This represents the average distribution of the bed materials for the study area. Also, a specific gravity test for the bed materials is performed according to ASTM D854-02 [17], where the average value of the specific gravity for the study area is 2.69.
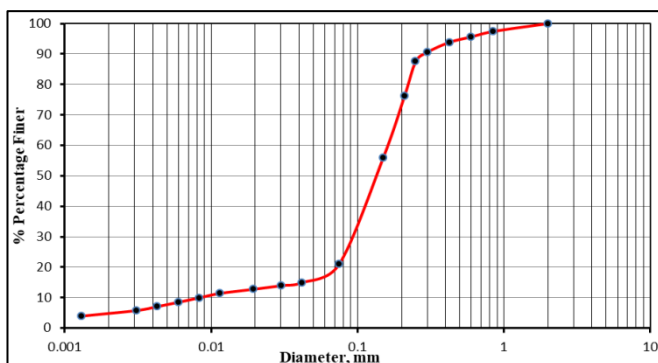

Fig. 5 Average of sieve analysis for all the sections.

5.3. Calculation of suspended sediment discharge

The suspended sediments discharge for the study area was calculated by multiplying the average suspended sediments concentration in the discharge of water and for each cross section by using the Eq. (24) [18]:

$$Qs = C \times Q \times 0.001 \tag{24}$$

Where: Qs is the discharge of suspended sediments in (kg/s), Q is the water discharge (m³/s), and C is the suspended sediment concentration (mg/l). The values range of the suspended sediments discharge for this study area and for the 20 cross-sections are 9 to 14.1 (kg/s).

6. The results obtained from the (SSIIM) model

The grid of (SSIIM) model for this study area consists of 1001 nodes in the x-direction, 21 nodes in y-direction and 11 nodes in z-direction, this depends on the size of the study area and the accuracy of the required results as shown in Fig. 6. The results of this model are divided into two parts. The first part concerning with the flow model, while the second part concerning with the sediment model.
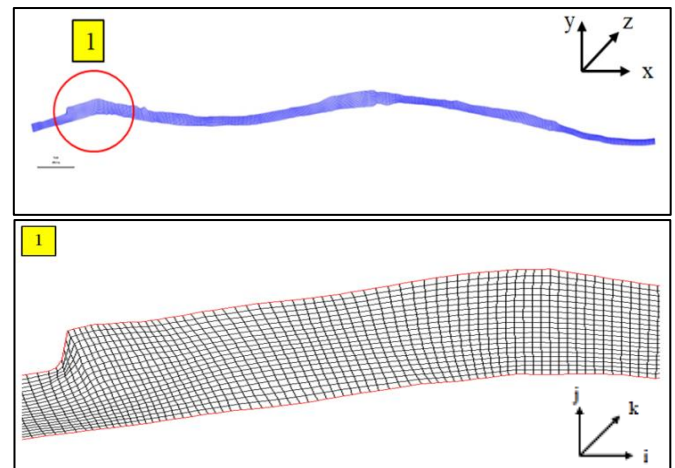

Fig. 6 Grid generated by (SSIIM) model for study reach.

6.1. Distribution of flow velocities (flow model)

The results of the flow velocity distribution obtained from the SSIIM model are divided into two parts. The first part included the velocity distribution in plane x-y. While the second part included the flow velocity distribution in plane y-z i.e. through the cross-sections, this in turn includes two types of flow velocity distributions: the first is the secondary flow as velocity vector, and the second is the distribution of flow velocity in the longitudinal direction i.e. with the direction of the main flow.

Figure 7 shows the distributions of flow velocity as a color gradient for the regions between section No. 1 to section No. 5 from the study area at levels 2 and 11 located near the water surface and near the river bed, respectively. It is clear from these figures that the maximum flow velocity occurs near the water surface and gradually decreases down to the river bed.

With regards to the distributions of flow velocity represented by the secondary flow in the y-z plane, the model results show that there is a deviation in the direction of the main flow due to the centrifugal force, which also occurs as a

result of bends in some sections of the study area. Figure 8 shows the secondary flow as velocity vectors with scale for section No. 14, where the arrows represent the value and direction of velocity compounds in the directions of *v* and *w* in the specified cross-section. As mentioned above, the secondary flow causes the deviation of the main flow direction from its path, which in turn causes the flow elements to be transported from the top of the surface to the bed thus causing increased erosion in some parts of the cross-sections.

Distribution of flow velocity through the cross-section and in plane *y-z*, but with the direction of the flow i.e. in the direction of *x*, is also one of the main results obtained during the simulation of the SSIIM model shown in Fig. 9 for cross-section No. 16 as a color gradient. The velocity is greatest at the surface of the water and decreases down to the river bed, reaching the lowest possible level. This result corresponds with the general velocity distribution scheme.
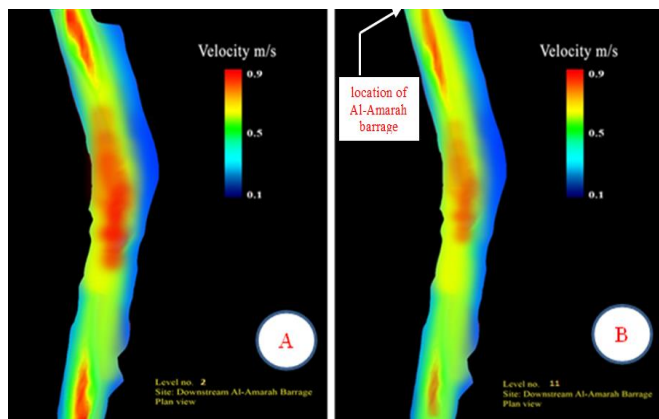

Fig. 7 The distribution of flow velocities in (*x-y*) plane, **(A)** at level 2 and **(B)** at level 11 for the regions between section No. 1 and section No. 5.
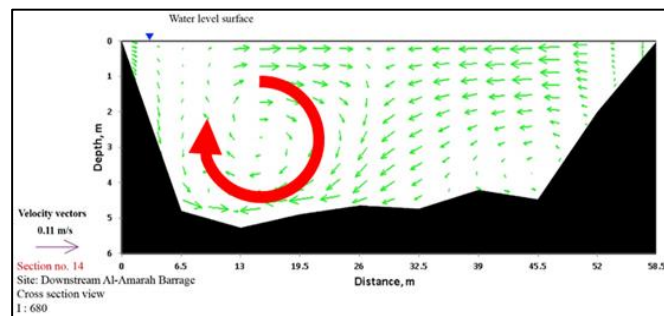

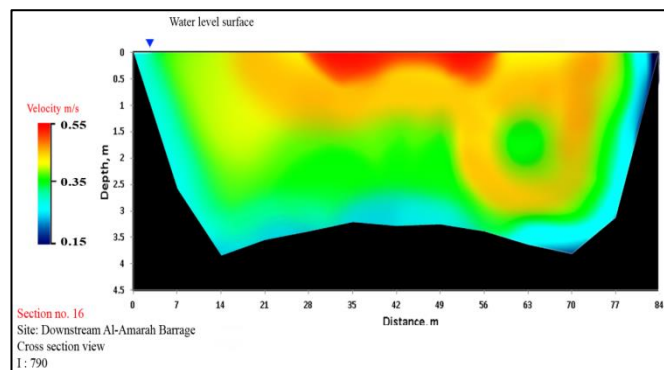**Fig. 8** Secondary flow at section No. 14 in (*y-z*) plane.

Fig. 9 Longitudinal velocity in *x*-direction as a color gradient for cross-section No. 16.

6.2. Distribution of suspended sediment (sediment model)

The results obtained from the SSIIM model show the concentrations of suspended sediments at the cross-sections i.e. in the *y-z* plane of the study area. It is obvious that, and as well known, the concentration of suspended sediments is high near the river bed and low near the water surface, as shown in Fig. 10 and Fig. 11. In addition, the concentrations of suspended sediments were higher near the sides of the cross-sections compared to the middle region. This is due to the decrease in flow velocity near the river bed which in turn increases the concentration of sediments in that area; vice versa, the flow velocity near the water surface is high thus causing the concentration of sediments to decrease. Another reason is due to the river bends which decrease the flow velocity thus causing an increase in sediment concentrations. These sediment data are important in understanding the sediment transport mechanism and knowledge of morphological changes in the river. The results obtained through the analysis of the SSIIM model help identify the sites where high concentrations of sediments occur in this study area. In turn, the Al-Amarah barrage administration and the management of water resources in the governorate of Maysan will have the needed data to take necessary measures in the future.
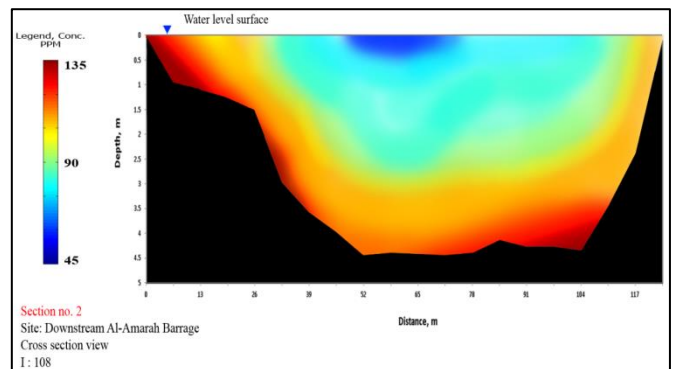

Fig. 10 Distributions of suspended sediment concentration as a color gradient at cross-section No. 2.
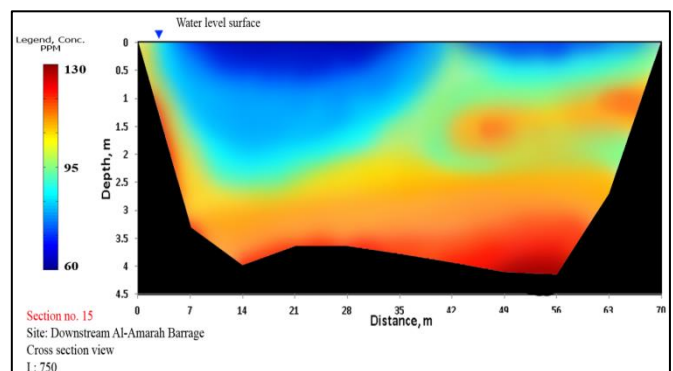

Fig. 11 Distributions of suspended sediment concentration as a color gradient at cross-section No. 15.

7. Verification from the results of the SSIIM model

The model results were verified by comparison with field measurements. The results verification is divided into two parts, the first relates to flow velocity calculations (flow model), and the second relates to suspended sediment concentrations (sediment model).

Major comparisons were carried out between the results of the model and the field measurements as well as between all calculations of flow velocity and suspended sediment concentrations, all cross-sections, and all the depths (i.e. 0.2*d*, 0.6*d* and 0.8*d*) for each column of the cross-section (i.e. *L*, *M*, and *R*). Satisfactory results were obtained through the comparisons between the results of the model and the field measurements. Figure 12 illustrates the comparison between the measured and calculated flow velocities for the case of 0.2*d* for *L*, *M*, and *R* and for all the cross-sections of the study area, where a good agreement is observed depending on determination coefficient (R^2) and which reaches between 0.87 and 0.96. Figure 13 illustrates the comparison between the values calculated by the SSIIM model and the field measurements of the suspended sediment concentrations for case 0.8*d* for *L*, *M*, and *R* as well as for all the cross-sections of the study area, it shows that satisfactory results are obtained with a determination coefficient (R^2) between 0.85 and 0.94. The difference between the field measurements and the model calculations for both flow velocity and sediment concentrations is caused by inaccuracies during measurements and reach geometry. Another reason for the deviation between the field-measured values and the model-calculated values is the cell size in the mathematical model. Therefore, appropriate decisions must be made regarding the number of grids in the three directions (*x*, *y*, and *z*) which are achieved through experience in numerical modeling.
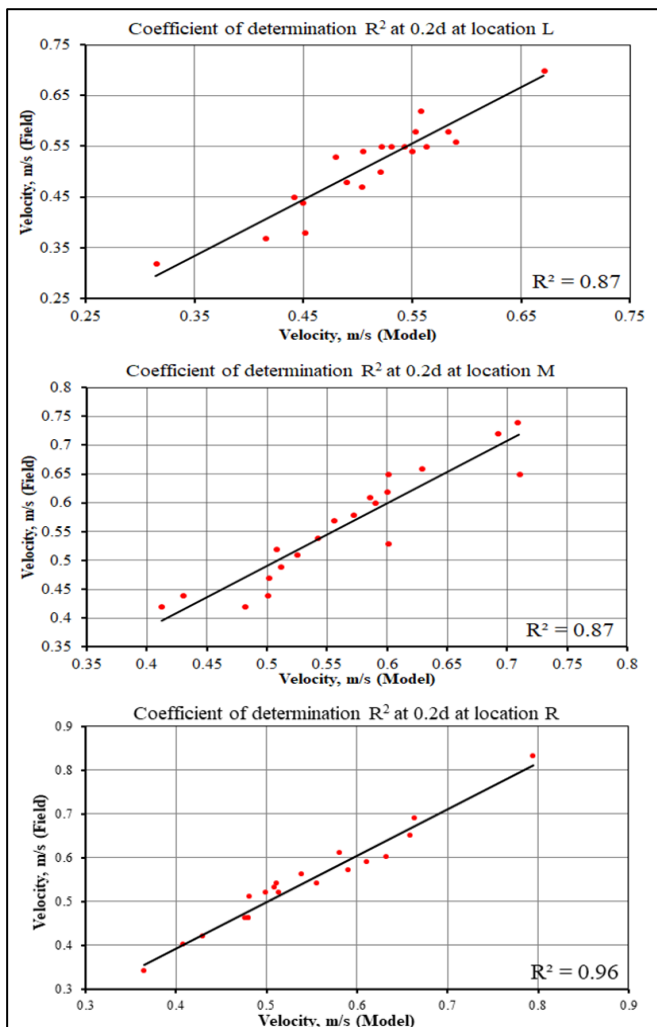

Fig. 12 The comparisons between the measured values and simulated values of velocities at 0.2*d* for (*L*, *M*, and *R*).
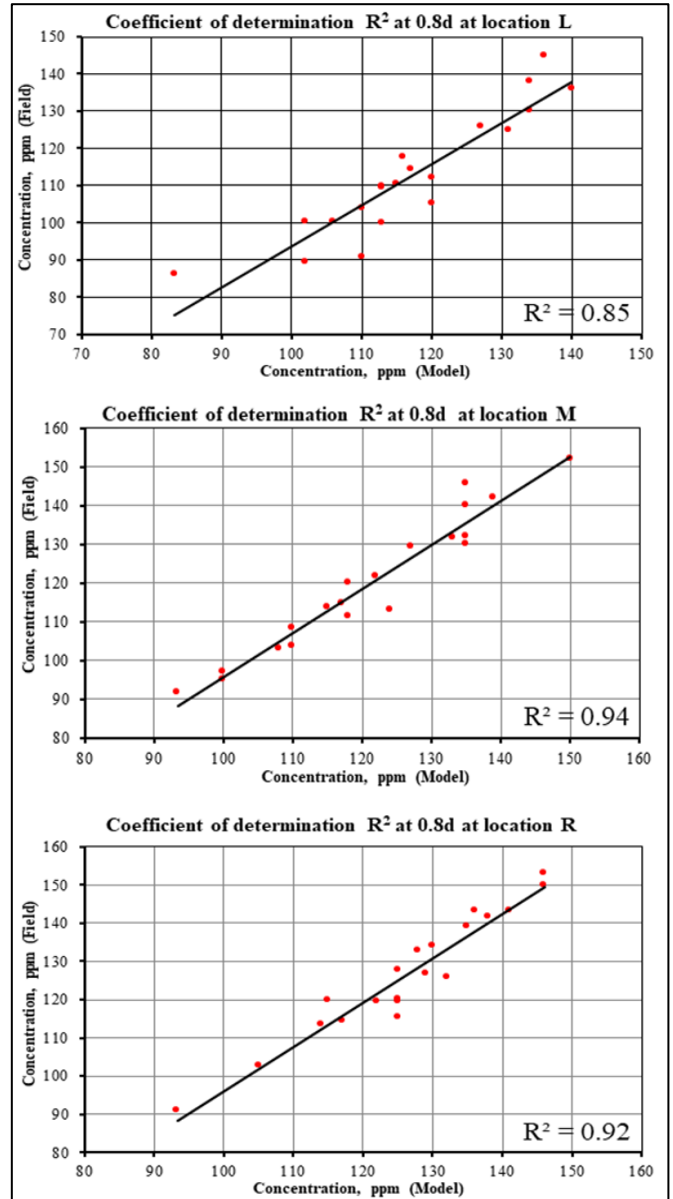

Fig. 13 The comparisons between the measured values and simulated values of sediment concentrations at 0.8*d* for (*L*, *M*, and *R*).

4. Conclusions

In this study, a three-dimensional model is prepared using the SSIIM software to simulate the flow and sediment transport on the study area located at the downstream of the Al-Amarah barrage within the Maysan province. And based on the results the following conclusions were drawn:

1. The secondary flow effects on both the main flow, sediment concentration, and the increase in erosion on the river bed. Where causes deviation of the main flow direction from its path, which in turn causes the flow elements to be transported from the top of the surface to the bed, thus causing increased erosion in some parts of the cross-sections.
2. The study showed, a good and real relationship between sediment transport and hydrodynamic processes where high sediment concentrations are observed at the lower velocities values and vice versa.
3. The results showed that the suspended sediment concentrations are large near the sides of the cross sections compared to the middle of the cross sections.

4. The simulation results and the measured data indicated that there is a problem in managing the transport of sediments, due to the large amounts of sediments in this study area, which requires conducting some studies on the possibility of construction some hydraulic projects related to reducing sediment transport to maintain the water quality, such as projects of sediment capture ponds, in addition establishment modern monitoring stations.

5. A good agreement obtained between the model's simulation results and the field measurements of flow velocity, as evident in case 0.2*d* for *L*, *M*, and *R* where the determination coefficient R^2 is between 0.87 and 0.96.

6. A good agreement obtained between the model's simulation results and the field measurements of suspended sediment concentrations, as evident in case 0.8*d* for *L*, *M*, and *R* where the determination coefficient R2 is between 0.85 and 0.94.

References

[1] H. Chanson, The hydraulics of open channel flow: an introduction, 2nd Edition, Elsevier, Butterworth-Heinemann, 2004.
https://doi.org/10.1016/B978-0-7506-5978-9.X5000-4

[2] A. Khosronejad, C. D. Rennie, S. A. A. S. Neyshabouri, and R. D. Townsend, "3D numerical modeling of flow and sediment transport in laboratory channel bends", ASCE, Journal of Hydraulic Engineering, Vol. 133, Issue 10, pp. 1123-1134, 2007.
https://doi.org/10.1061/(ASCE)0733-9429(2007)133:10(1123)

[3] A. H. A. Atya, "Open channel flow simulation (sedimentation problem in rosaries dam)", M.Sc. thesis, University of Khartoum, Faculty of Engineering, 2008.

[4] A. A. Ali, N. A. Al-Ansari, Q. Al-Suhail, and S. Knutsson, "Three-dimensional morphodynamic modelling of Tigris river in Baghdad", Journal of Civil Engineering and Architecture, Vol. 11, pp. 571-594, 2017.
https://doi.org/10.17265/1934-7359/2017.06.005

[5] M. E. Mohammad, N. A. Al-Ansari, S. Knutsson, and J. Laue, "A computational fluid dynamics simulation model of sediment deposition in a storage reservoir subject to water withdrawal", MDPI, Water Journal, Vol. 12, Issue 4, pp. 1-15, 2020.
https://doi.org/10.3390/w12040959

[6] N. R. B. Olsen, "A three-dimensional numerical model for simulation of sediment movements in water intakes with multiblock option", SSIIM User's Manual. Department of Civil and Environmental Engineering, Norwegian University of Science and Technology, 2018.

[7] K. R. Abed, M. H. Hobi, and A. J. Jihad, "Numerical modeling of sediment transport upstream of Al-Ghammas barrage", International Journal of Scientific & Engineering Research, Vol. 5, Issue 11, pp. 469-477, 2014.

[8] B. E. Launder and D. B. Spalding, "The numerical computation of turbulent flows", Computer Methods in Applied Mechanics and Engineering, Vol. 3, Issue 2, pp. 269-289, 1974.
https://doi.org/10.1016/0045-7825(74)90029-2

[9] B. E. Launder, A. Morse, W. Rodi, and D. B. Spalding, "Prediction of free shear flows: a comparison of the performance of six turbulence models", Imperial College of Science and Technology, London, United Kingdom, Vol. 1, pp. 361-426, 1972.

[10] H. Schlichting, Boundary-Layer Theory, 7th Edition, Engineering University of Braunachwcig, Germany, McGraw-Hill Book Company, 1979.

[11] L. C. Van Rijn, "Mathematical modelling of morphological processes in the case of suspended sediment transport", Ph.D. thesis, published as Delft Hydraulics Communication No. 382, Civil Engineering and Geosciences, 1987.
http://resolver.tudelft.nl/uuid:c1c1fce6-afc6-4ca3-b707-e108f256048c

[12] Eijkelkamp Soil and Water, Van veen grabs manual. Giesbeek, the Netherlands, 2008.

[13] A. A. Adegbola and O. S. Olaniyan, "Estimation of bed load transport in river Omi, south western Nigeria using grain size distribution data", International Journal of Engineering and Technology, Vol. 2, No. 9, pp. 1587-1592, 2012.

[14] J. S. Maatooq, H. A. Omran, and H. K. Aliwe, "Empirical formula for estimation the sediment load in shat Al-Gharaf river", Basrah Journal for Engineering Sciences, Vol. 16, No. 1, pp. 38-41, 2016.
https://www.iasj.net/iasj/download/8aff54ee3b4bdf8e

[15] Inter-Agency Committee on Water Resources, "A study of methods used in measurement and analysis of sediment loads in streams", Report NO. 14. Determination of Fluvial Sediment Discharge, 1963.

[16] ASTM Standards D 422-63, "Standard test method for particle-size analysis of soils", ASTM International Committee on Soil and Rock, United States, 2007.

[17] ASTM Standards D 854-02, "Standard test methods for specific gravity of soil solids by water pycnometer", ASTM International Committee on Soil and Rock, United States, 2002.

[18] D. R. Maidment, Handbook of hydrology, 1st Edition, Civil Engineering, University of Texas at Austin, McGraw-Hill Company, New York, 1993.